ACS SYMPOSIUM SERIES 418

Marine Toxins

Origin, Structure, and Molecular Pharmacology

Sherwood Hall, EDITOR
U.S. Food and Drug Administration

Gary Strichartz, EDITOR
Brigham and Women's Hospital
Harvard Medical School

Developed from a symposium held ... in Woods Hole, Massachusetts, under the auspices of the International Union of Pure and Applied Chemistry, and sponsored through an interagency agreement between the U.S. Army Medical Research Institute of Infectious Diseases and the Center for Food Safety and Applied Nutrition, U.S. Food and Drug Administration

American Chemical Society, Washington, DC 1990

Chapter 12

Detection, Metabolism, and Pathophysiology of Brevetoxins

Mark A. Poli, Charles B. Templeton, Judith G. Pace, and Harry B. Hines

Pathophysiology Division, U.S. Army Medical Research Institute of Infectious Diseases, Fort Detrick, Frederick, MD 21701–5011

Methods of detection, metabolism, and pathophysiology of the brevetoxins, PbTx-2 and PbTx-3, are summarized. Infrared spectroscopy and innovative chromatographic techniques were examined as methods for detection and structural analysis. Toxicokinetic and metabolic studies for in vivo and in vitro systems demonstrated hepatic metabolism and biliary excretion. An in vivo model of brevetoxin intoxication was developed in conscious tethered rats. Intravenous administration of toxin resulted in a precipitous decrease in body temperature and respiratory rate, as well as signs suggesting central nervous system involvement. A polyclonal antiserum against the brevetoxin polyether backbone was prepared; a radioimmunoassay was developed with a sub-nanogram detection limit. This antiserum, when administered prophylactically, protected rats against the toxic effects of brevetoxin.

Red tides resulting from blooms of the dinoflagellate *Ptychodiscus brevis* in the Gulf of Mexico have elicited a great deal of scientific interest since the first documented event over 100 years ago (*1*). Human intoxications from the ingestion of contaminated shellfish and the impact of massive fish kills on the tourist industry along the Gulf coast of the United States have resulted in a concerted research effort to understand the genesis of red tides and to isolate and characterize the toxins of *P. brevis*.

Research in this area advanced in the 1970's as several groups reported the isolation of potent toxins from *P. brevis* cell cultures (*2–7*). To date, the structures of at least eight active neurotoxins have been elucidated (PbTx-1 through PbTx-8) (*8*). Early studies of toxic fractions indicated diverse pathophysiological effects in vivo as well as in a number of nerve and muscle tissue preparations (reviewed in 9–11). The site of action of two major brevetoxins, PbTx-2 and PbTx-3, has been shown to be the voltage-sensitive sodium channel (*8,12*). These compounds bind to a specific receptor site on the channel complex where they cause persistent activation, increased Na^+ flux, and subsequent depolarization of excitable cells at resting

membrane potentials. At present, the brevetoxins are the only ligands unequivocally demonstrated to act at this site (neurotoxin receptor site 5), although mounting evidence (*13*) suggests the toxins involved in ciguatera intoxication also may bind there.

We are investigating low-molecular-weight toxins of animal, plant, and microbial origin. Our goals are to develop methods to detect these compounds in both environmental and biological samples and to develop prophylaxis and treatment regimens. This chapter summarizes the results of our current investigations of the brevetoxins. Some of these studies will be published elsewhere in greater detail.

Chemical Detection and Stability

A variety of chromatographic and spectrographic techniques have been applied to the study of the brevetoxins. High performance liquid chromatography (HPLC) and thin-layer chromatography (TLC) were instrumental in the initial isolation and purification processes. Mass spectrometry (MS), infrared spectroscopy (IR), circular dichroism (CD), nuclear magnetic resonance spectroscopy (NMR), and X-ray crystallography all played important roles in structure determinations. As research efforts expand to include metabolic studies, these techniques become increasingly important for detection and quantification of exposure as well as structural elucidation of metabolites.

Chromatography. A number of HPLC and TLC methods have been developed for separation and isolation of the brevetoxins. HPLC methods use both C18 reversed-phase and normal-phase silica gel columns (*8, 14, 15*). Gradient or isocratic elutions are employed and detection usually relies upon ultraviolet (UV) absorption in the 208–215-nm range. Both brevetoxin backbone structures possess a UV absorption maximum at 208 nm, corresponding to the enal moeity (*16,17*). In addition, the PbTx-1 backbone has an absorption shoulder at 215 nm corresponding to the γ-lactone structure. While UV detection is generally sufficient for isolation and purification, it is not sensitive (>1 ppm) enough to detect trace levels of toxins or metabolites. Excellent separations are achieved by silica gel TLC (*14, 15, 18-20*). Sensitivity (>1 ppm) remains a problem, but flexibility and ease of use continue to make TLC a popular technique.

Mass Spectrometry. Mass spectrometry holds great promise for low-level toxin detection. Previous studies employed electron impact (EI), desorption chemical ionization (DCI), fast atom bombardment (FAB), and cesium ion liquid secondary ion mass spectrometry (LSIMS) to generate positive or negative ion mass spectra (*15-17, 21–23*). Firm detection limits have yet to be reported for the brevetoxins. Preliminary results from our laboratory demonstrated that levels as low as 500 ng PbTx-2 or PbTx-3 were detected by using ammonia DCI and scans of 500–1000 amu (unpublished data). We expect significant improvement by manipulation of the DCI conditions and selected monitoring of the molecular ion or the ammonia adduction.

The success of the soft ionization techniques (DCI, FAB, and LSIMS) presents several possibilities for detection of brevetoxins in complex matrices. Positive-ion DCI was used for the analysis of PbTx-3 metabolites generated in vitro by isolated rat hepatocytes (see below). Unmetabolized parent was conclusively identified and metabolites were tentatively identified, pending confirmation by alternate methods (see below).

Chemical Stability and Decontamination. The stability of the brevetoxins is of great interest from the standpoints of detection, metabolism, and safety. PbTx-2 and PbTx-3 have been investigated in our laboratories in order to design rational safety

protocols for toxin handling and disposal of contaminated waste (*24;* R.W. Wannamacher, unpublished data). These compounds were stable for months when stored in the refrigerator either dry or in organic solvents such as ethanol, methanol, acetone, or chloroform. However, toxins with the PbTx-1 backbone have been reported to be unstable in alcohol (*15*). PbTx-2 and PbTx-3 were unstable at pH values less than 2 and greater than 10, in the presence of 50 ppm chlorine, and at temperatures greater than 300°C. For decontamination of laboratory glassware and surfaces, greater than 99% of the detectable brevetoxin was destroyed by a 10-min exposure to 0.1 N NaOH. Disposable waste can be incinerated if the combustion chamber temperature reaches at least 300°C. Autoclaving was shown to be ineffective for decontamination (*24*).

Distribution and Metabolic Fate—In Vivo and In Vitro Studies

Of particular interest in brevetoxin research are the diagnosis of intoxication and identification of brevetoxins and their metabolites in biological fluids. We are investigating the distribution and fate of radiolabeled PbTx-3 in rats. Three model systems were used to study the toxicokinetics and metabolism of PbTx-3: 1) rats injected intravenously with a bolus dose of toxin, 2) isolated rat livers perfused with toxin, and 3) isolated rat hepatocytes exposed to the toxin in vitro.

In the first study, male Sprague-Dawley rats (300–350 g) were given an intravenous bolus of [^{3}H]PbTx-3 (9.4 Ci/mmol, 6 μg/kg body weight) via the penile vein (*25*). The plasma concentration curve (Figure 1) was bi-exponential with a rapid distribution phase (half-life approx. 30 sec) and a slower elimination phase (half-life = 112 min). Toxin clearance (dose administered/area under the plasma concentration curve) in the whole animal was 0.23 ml/min/g liver. In a 325-g rat, hepatic blood flow (Q) is 13.2 ml/min (*26*), and, assuming hepatic clearance was equal to mean total clearance (Cl), the calculated in vivo extraction ratio (Cl/Q) was 0.55. Within 1 min, 94% of the administered toxin had distributed to the tissues. After 30 min, the liver contained 16%, skeletal muscle 70%, and the gastrointestinal tract 8% of the administered radioactivity. The heart, kidneys, testes, brain, lungs, and spleen each contained less than 1.5%. By 24 hr, radioactivity in skeletal muscle decreased to 20% of the total administered dose. Over the same period, radioactivity remained constant in the liver and increased in the stomach, intestines, and feces, suggesting biliary excretion was an important route of toxin elimination. By day 6, 89% of the total radioactivity had been excreted in the urine and feces in a ratio of 1:5. TLC analysis of urine (Figure 2) and feces indicated that the parent toxin had been metabolized to several more polar compounds.

To further investigate the role of the liver in brevetoxin metabolism, PbTx-3 was studied in the isolated perfused rat liver model (*27, 28*). Radiolabeled PbTx-3 was added to the reservoir of a recirculating system and allowed to mix thoroughly with the perfusate. Steady-state conditions were reached within 20 min. At steady-state, 55–65% of the delivered PbTx-3 was metabolized and/or extracted by the liver; 26% remained in the effluent perfusate. Under a constant liver perfusion rate of 4 ml/min, the measured clearance rate was 0.11 ml/min/g liver. The calculated extraction ratio of 0.55 was in excellent agreement with the in vivo data. Radioactivity in the bile accounted for 7% of the total radiolabel perfused through the liver. PbTx-3 was metabolized and eliminated into bile as parent toxin plus four more-polar metabolites (Figure 3). Preliminary results of samples stained with 4-(*p*-nitrobenzyl)-pyridine (*29*) indicated the most polar metabolite was an epoxide.

In vitro metabolism of [^{3}H]PbTx-3 was studied in isolated rat hepatocytes (*25*). Hepatocyte monolayers cultured in 6-well plates containing 1 ml modified Williams E medium were incubated with 0.1 μg radiolabeled toxin at 37°C for 24 hr. The

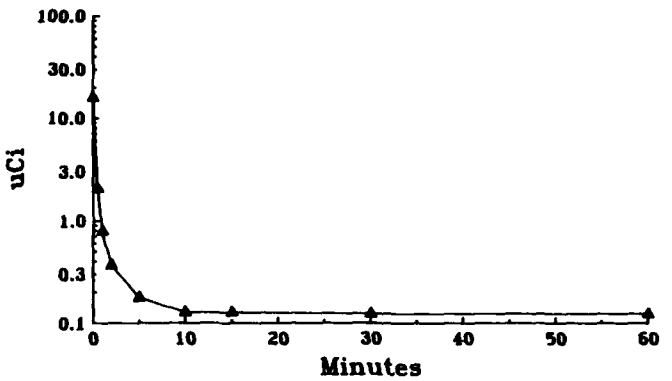

Figure 1. Semilogarithmic plot of brevetoxin (μCi) in plasma over time after an intravenous injection of tritium-labeled PbTx-3. T 1/2 alpha = 30 sec; T 1/2 beta = 112 min.

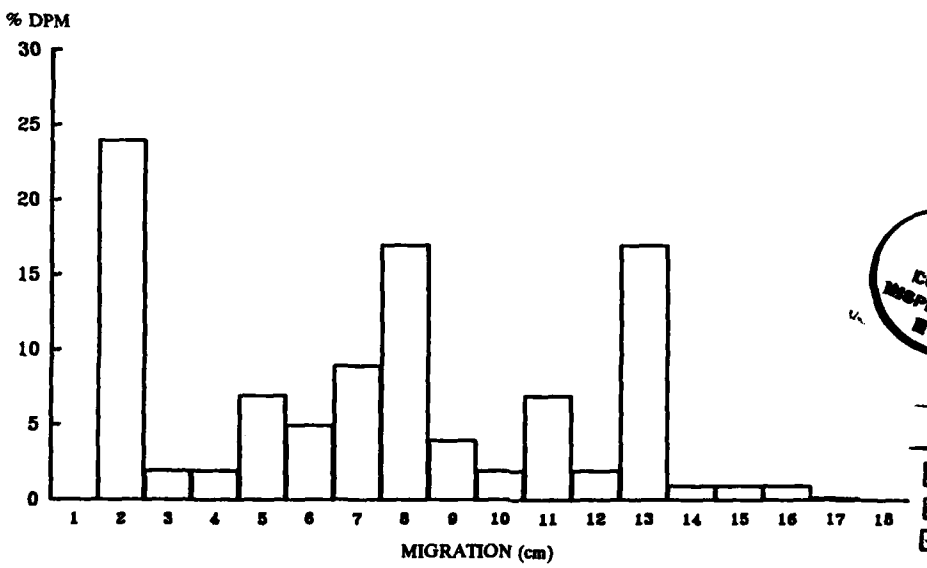

Figure 2. Thin-layer radiochromatogram of urine (100 μl) from rats injected with labeled PbTx-3. TLC plates were developed in two sequential solvent systems: chloroform:ethyl acetate:ethanol (50:25:25; 80:10:10). Radioactive zones were scraped and counted in a liquid scintillation counter. Native PbTx-3 runs at 13 cm.

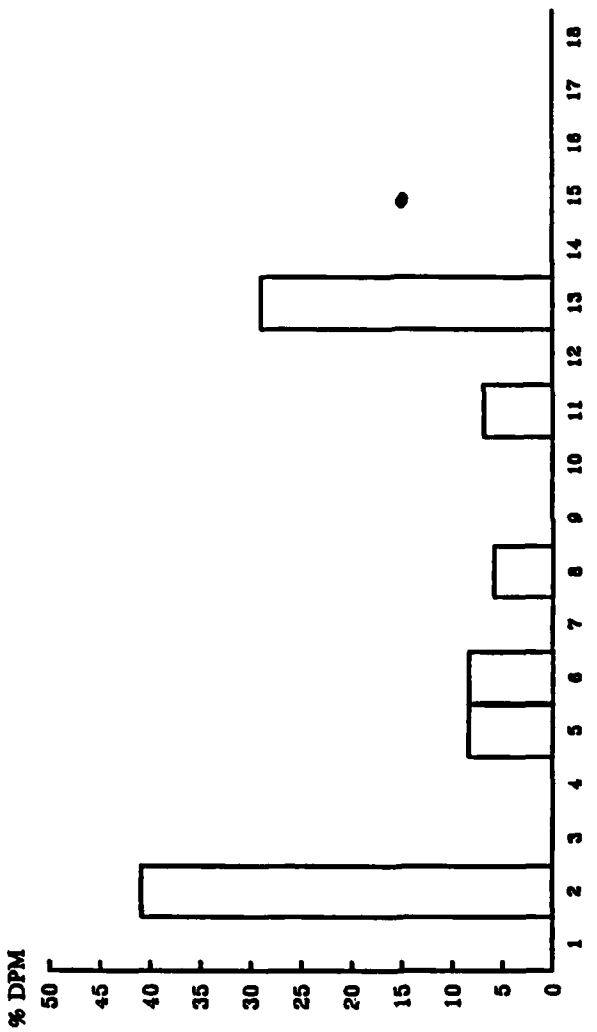

Figure 3. Thin-layer radiochromatogram of bile (1 hr). Aliquots of bile (20 μl) were analyzed by TLC by two sequential solvent systems of chloroform:ethyl acetate:ethanol (50:25:25; 80:10:10). Native PbTx-3 runs at 13 cm.

cell culture medium was sampled periodically during the incubation and analyzed for labeled metabolites via HPLC. The hepatocytes metabolized PbTx-3 to at least three metabolites that exhibited greater polarity than the parent toxin and corresponded closely in relative polarity to the major metabolites obtained in vivo and from the isolated perfused liver. In addition, a fourth peak appeared after approximately 20 min (Figure 4). From preliminary results, it is not clear whether this fourth peak was related to cellular metabolism. The differences in metabolite profiles between this system and the bile produced by the isolated perfused liver are under investigation. Two of the three metabolites generated in vitro cross-reacted strongly with our anti-PbTx antiserum (see below), suggesting conservation of at least a portion of the native backbone structure (data not shown).

By applying an extension of the clearance concept (*30, 31*), in vitro metabolism was used to predict in vivo toxin elimination. Hepatocytes were incubated with 0.5 to 10 μg unlabeled PbTx-3 containing 0.1 μg radiolabeled toxin as tracer. Disappearance of parent compound and the appearance of metabolites were measured by HPLC equipped with a Radiomatic isotope detector. V_{max} (1.6 nmol/min/g liver) and K_m (8.56 μM) were determined by non-linear regression. Intrinsic clearance (V_{max}/K_m) was 0.15 ml/min/g liver and the calculated hepatocyte extraction ratio, 0.46, again was in good agreement with the in vivo data.

These studies represent the first report of the metabolism of brevetoxins by mammalian systems. PbTx-3 was rapidly cleared from the bloodstream and distributed to the liver, muscle, and gastrointestinal tract. Studies with isolated perfused livers and isolated hepatocytes confirmed the liver as a site of metabolism and biliary excretion as an important route of toxin elimination. [^{3}H]PbTx-3 was metabolized to several compounds exhibiting increased polarity, one of which appeared to be an epoxide derivative. Whether this compound corresponds to PbTx-6 (the 27,28 epoxide of PbTx-2), to the corresponding epoxide of PbTx-3, or to another structure is unknown. The structures of these metabolites are currently under investigation.

Data from both in vivo and in vitro systems showed PbTx-3 to have an intermediate extraction ratio, indicating in vivo clearance of PbTx-3 was equally dependent upon liver blood flow and the activity of toxin-metabolizing enzymes. Studies on the effects of varying flow rates and metabolism on the total body clearance of PbTx-3 are planned. Finally, comparison of in vivo metabolism data to those derived from in vitro metabolism in isolated perfused livers and isolated hepatocytes suggested that in vitro systems accurately reflect in vivo metabolic processes and can be used to predict the toxicokinetic parameters of PbTx-3.

Pathophysiological Effects of PbTx-2 in Conscious Rats

The pathophysiological effects of PbTx-2 were examined in the conscious, tethered rat (*32*). This is the model of choice because neurological and behavioral responses can be characterized without interference from anesthetic effects. Male rats (Sprague-Dawley, 350–500 g) were anesthetized with 55 mg/kg pentobarbital and placed on a heated surgical board. A catheter, placed into the carotid artery and advanced until the distal tip resided in the aorta, was used to measure arterial blood pressure and to sample blood for blood gas measurements. Another catheter, placed into the jugular vein and advanced until the distal tip was near the cranial vena cava, was used for experimental infusions. Thermistor probes were implanted into the abdominal cavity and subcutaneously over the sternum. Electrocardiograph (ECG) leads were placed subcutaneously over the ventral and dorsal thorax to obtain a V10 tracing. All lead wires and catheters were tunneled subcutaneously to the dorsal cervical area and passed through a 20-cm steel spring tether. Catheters

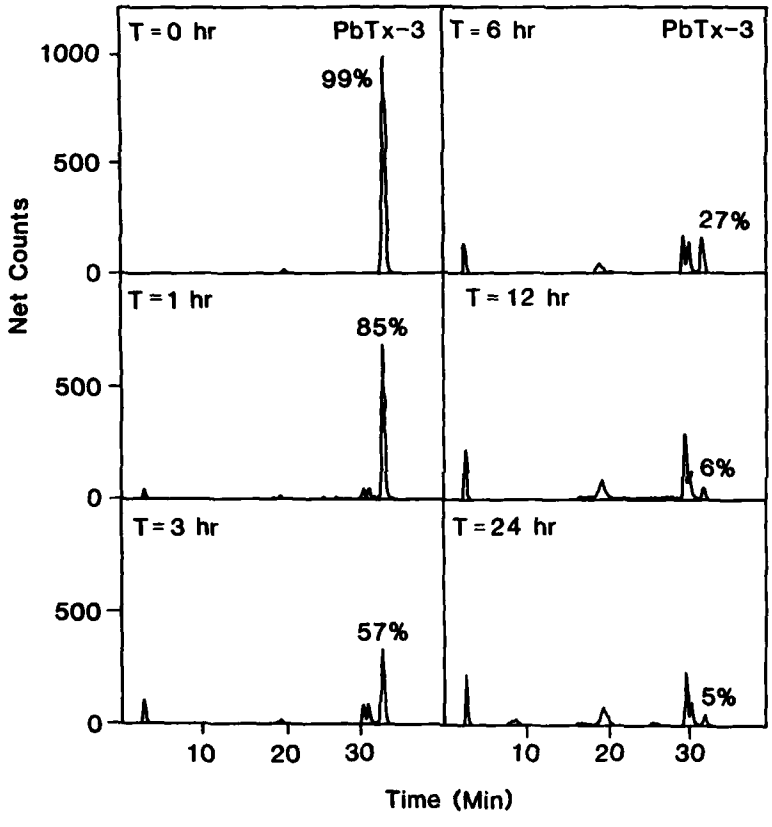

Figure 4. C18 reverse-phase HPLC radiochromatogram of PbTx-3 and metabolites in hepatocyte media (50 μl) over 24 hr. Nonlinear gradient of methanol:water; flow rate = 1 ml/min.

were then flushed with heparinized saline and plugged with stainless steel pins. The animals were placed in cages and the tether passed through the wire mesh cage top to allow sampling. After recovery from anesthesia, the rats were able to move freely about the cage while being monitored; sampling was conducted without perturbing the animals.

The initial phase of the study focused on determining a route of toxin administration that would result in sublethal toxic effects. Intravenous, intraarterial, intraperitoneal, and subcutaneous bolus injections were examined. With the exception of the subcutaneous route, bolus injections of greater than 200 μg/kg resulted in total body paralysis, shock, and death within 2–3 min. Onset was so rapid that the animals often entered paralysis during the several seconds required to complete the bolus injection. Doses of 100 μg/kg or greater resulted in rapid-onset cardiac and respiratory paralysis and death within 5–10 min. With lower, non-lethal, intravascular or intraperitoneal doses (≤25 μg/kg), rats showed immediate cardiac and respiratory effects, but compensation occurred within 5–10 min. There were no apparent skeletal muscle contractions in these lower-dose animals. Both subcutaneous and intraperitoneal administration caused sustained effects, but responses varied among animals. However, when rats were slowly infused intravenously at doses of ≤100 μg/kg over 1 hr, animal-to-animal variation decreased markedly and responses were sustained for a longer time. Therefore, to allow sufficient monitoring time and to minimize variations among animals, a 1-hr intravenous infusion was chosen for all subsequent studies.

To characterize the responses to PbTx-2, five dose rates (0, 12.5, 25, 50, and 100 μg/kg/hr in 2 ml saline) were infused into the jugular catheters of rats (four per group). Heart rates, systolic and diastolic arterial blood pressures, pulse pressures, respiratory rates, core and peripheral body temperatures, lead V10 ECGs, and arterial blood gases were monitored. Clinical signs and behaviors were recorded by video camera. After infusion, animals were monitored for 6 hr, by which time most had either died or recovered to near baseline physiological levels.

All rats infused with 100 μg/kg PbTx-2 died within 2 hr. Only one rat infused with 50 μg/kg died during the 6-hr study. All other animals survived. The calculated 6-hr LD_{50} for this study of 20 animals given a 1-hr intravenous infusion of PbTx-2 was 60 μg/kg. Since all of the rats given 50 μg/kg by bolus injection died very early, it is evident that the LD_{50} is lower if the toxin is given intravascularly by bolus injection.

The most dramatic change occurred in the respiratory rates. Upon the beginning of infusion, there was an immediate, precipitous, dose-dependent decrease in respiratory rates (Figure 5). The respiratory rates of the three highest dose groups fell to 20% of baseline. Except for the terminal values of the high-dose group, the blood gas analyses indicated a compensatory response that yielded insignificant changes in pO_2, pCO_2, HCO_3, base excess, pH, and total CO_2 during the entire 6-hr study. The 100 μg/kg group displayed typical terminal hypoventilation: hypercarbia, acidosis, and low oxygen tension (data not shown). Clinically, the animals ventilated very deeply, indicating much larger tidal volumes. All survivors had respiratory rates within the normal range within 6 hr, except the 50 μg/kg group, which recovered to only about 60% of baseline.

Each treatment group showed a dose-dependent decrease in core (Figure 6) and peripheral (not shown) body temperatures. The three highest dose groups decreased 1.5–2.0 degrees centigrade. The decrease in the lowest dose group averaged 0.5 degrees. In all groups, the decrease occurred during the infusion period. In the 50 μg/kg group, survivors showed no significant recovery during the 6-hr study. This simultaneous drop in core and peripheral body temperature may reflect decreased oxygen consumption and reduced heat production.

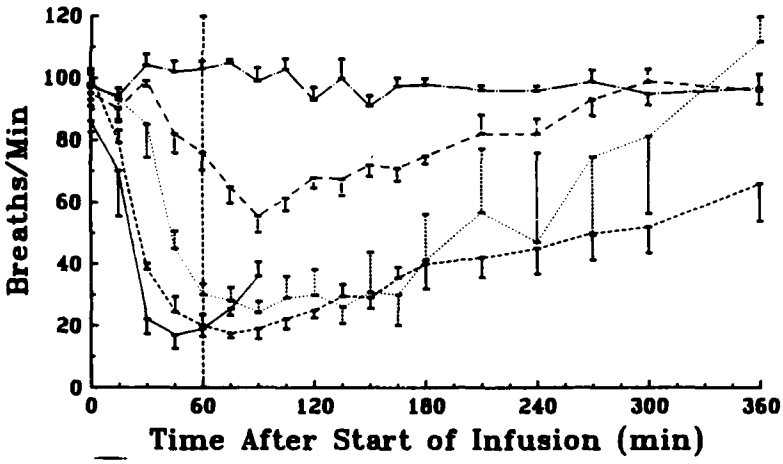

Figure 5. Dose–response curve of respiratory rate for rats given 1-hr infusion of PbTx-2. [____ = 100 μg/kg; --- = 50 μg/kg; . . . = 25 μg/kg; — — — = 12.5 μg/kg; —.— = 0 μg/kg.]

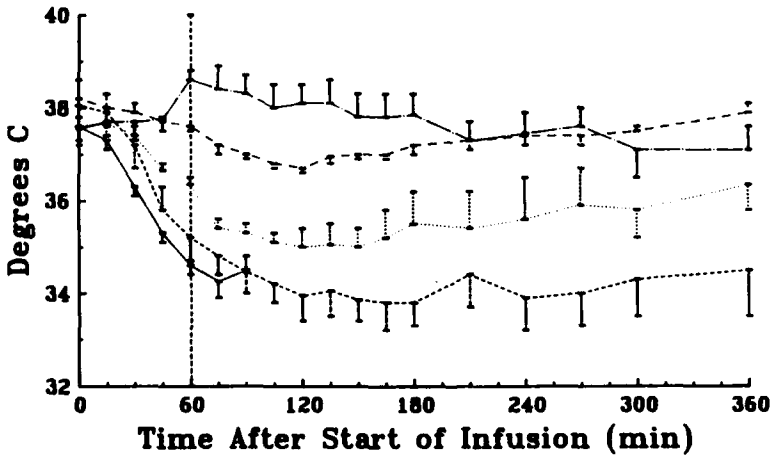

Figure 6. Dose–response curve of core temperature for rats given 1-hr infusion of PbTx-2. [____ = 100 μg/kg; --- = 50 μg/kg; . . . = 25 μg/kg; — — — = 12.5 μg/kg; —.— = 0 μg/kg.]

The lead V10 ECG indicated conduction defects in the Purkinje system of the heart. Numerous arrhythmias were recorded, including premature ventricular depolarizations, paroxysmal ventricular tachycardia, and complete heart block (Figure 7). Heart rates were not significantly altered, however, except in the 100 μg/kg group (data not shown). Systolic and diastolic arterial blood pressures did not change significantly in the higher-dose groups, but pulse pressures increased, suggesting compensation by increased cardiac outputs due to increased stroke volumes. Failure to maintain baseline heart rate and arterial pressure was seen in the 100 μg/kg group just before death, when the animals showed signs of complete cardiorespiratory collapse.

Rats administered PbTx-2 exhibited numerous and varied clinical signs. Consistent in all animals were gasping-like respiratory movements, head-bobbing, depression, and ataxia, all of which could be originating in the brain stem. Time of onset varied, but depression and gasping movements were generally the first clinical manifestations of intoxication. Head-bobbing and ataxia usually began 2-3 hr after infusion. These signs, coupled with the decrease in core temperature, suggested central nervous system involvement, and, more specifically, the brain stem and cerebellum. This conclusion was sustained in later studies when several animals developed head-tilt, a condition indicative of central nervous system involvement. In some animals, an apparently uncontrolled muscular contraction occurred, usually in the hindquarters, which caused the animals to lunge violently across the cage in one coordinated motion. Both hindquarters contracted simultaneously, indicating the initiating impulse originated at the level of the spinal cord or higher. This movement and head-bobbing are indicative of cerebellar involvement. All control animals sustained normal physiological parameters, ECG's, and behavior.

In summary, intravenous infusion of PbTx-2 caused toxic signs indicative of central nervous system involvement, including a precipitous fall in core and peripheral body temperatures and clinical signs of dysfunction that could be originating in the motor cortex, the cerebellum, or the spinal cord. The profound decreases in respiratory and heart rates could be peripherally mediated; these changes were detrimental only in the highest dose group animals. Compensation for the rate changes in the surviving animals occurred to an extent that blood gases and blood pressures were essentially normal.

Radioimmunoassay and Immunoprophylaxis

The ability to treat brevetoxin intoxication is dependent upon diagnosis and quantifying exposure. Currently, neither an effective, specific treatment nor a reliable assay for exposure to the brevetoxins exists. We prepared a specific antiserum against the brevetoxins and evaluated its use in an assay for exposure to the brevetoxins and in the treatment and prophylaxis of intoxication.

A toxin-bovine serum albumin (BSA) conjugate was prepared by succinylation of the alcohol function of PbTx-3, followed by standard carbodiimide coupling of the PbTx-3 hemisuccinate to the lysine residues of BSA (*33*). Fresh conjugate was prepared every two weeks to avoid decomposition; the molar ratios of toxin:BSA conjugate ranged from 7–14. Aliquots of conjugated toxin containing 0.25–0.50 mg equivalents of toxin in Freund's adjuvant were administered intramuscularly to an adult female goat. Blood samples were taken at weekly intervals, beginning at week 8, and analyzed for anti-PbTx-3 binding activity by standard radioimmunoassay.

Anti-PbTx antibodies appeared rapidly in the goat serum after the initial immunization. By the first bleed at week 8, binding capacity was approximately 0.5 nmol PbTx-3/ml serum, where it remained constant for several weeks. After cessation of boosts at week 10, the serum titers remained elevated for 6 weeks before

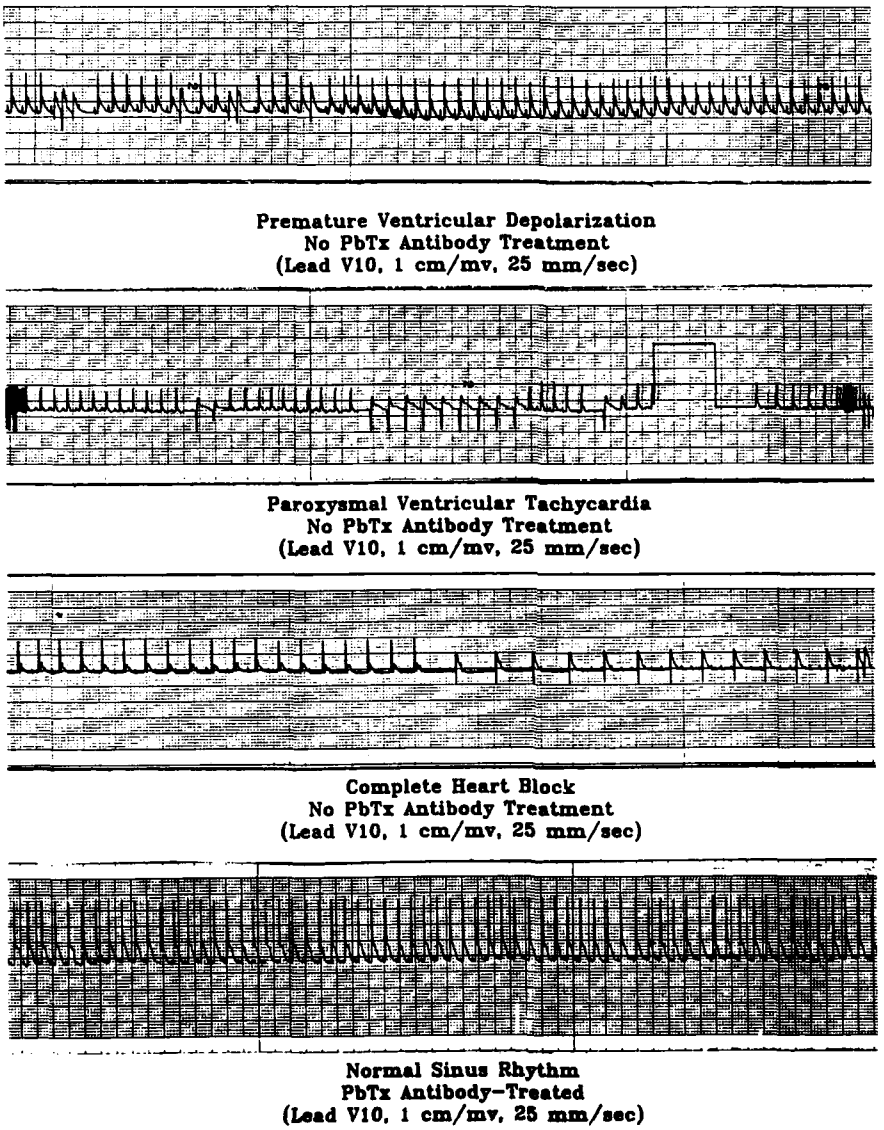

Figure 7. Electrocardiograms of rats at 30 to 90 min after beginning a 1-hr infusion of PbTx-2 (25 μg/kg). Bottom tracing is a representative ECG of a normal rat.

falling to very low levels by week 21. Resuming boosts at this time caused an immediate rebound in binding capacity to approximately 1.0 nmol/ml. Ammonium sulfate precipitation of the serum at week 22 resulted in ≥85% of the anti-PbTx-3 binding capacity precipitating with the serum IgG fraction. Rosenthal analyses of saturation curves before and after precipitation indicated a single class of high-affinity antibodies with an apparent affinity constant (K_d) of 1 nM (0.5–2.1, n=11) (data not shown).

Standard curves performed under our defined radioimmunoassay conditions ([^{3}H]PbTx-3 = 1 nM, antiserum dilution = 1:2000, assay volume = 1 ml) demonstrated the ability of this antiserum to bind equally to PbTx-2 and PbTx-3, suggesting specificity for the cyclic polyether backbone region of the molecule (Figure 8). The linear portion of the curve indicated a lower detection limit of 0.2–0.5 ng in saline buffer under these conditions. Evaluation of this assay for use with biological fluids and tissue extracts is underway.

After initial experiments demonstrating that the antiserum was capable of completely inhibiting the binding of [^{3}H]PbTx-3 to its receptor site in rat brain membranes (Figure 9), we began studies designed to evaluate potential of the antiserum for prophylaxis and treatment of brevetoxin intoxication (*34*). The tethered rat model was used, and surgical implantations were identical to those described above. Heart rate, core and peripheral body temperatures, lead V10 ECG, and arterial blood pressure were monitored continuously. Respiratory rate was recorded each 5 min for the first 3 hr, then each 15 min until 6 hr.

Conscious rats were pretreated with a 10-min infusion of anti-PbTx antiserum (25 mg/kg total protein, calculated PbTx binding capacity 0.29 nmol) or saxitoxin (control) antibody matched for total protein content. Twenty minutes after completion of the antisera infusion, brevetoxin (25 μg/kg, 28 nmol) was infused over 1 hr. Rats pretreated with control antiserum showed signs consistent with our pathophysiological characterization of brevetoxin intoxication at this dose: decreased respiratory rate, reduction in core and peripheral body temperatures, and cardiac arrhythmias. Arterial blood pressures and heart rates were variable. Rats treated with anti-PbTx antiserum showed no decrease in temperatures (Figure 10), no significant decreases in respiratory (Figure 11) or heart rates, and normal ECG's (Figure 7). Our antiserum was thus capable of blocking the in vivo effects of intravenously administered PbTx-2 under these conditions. Experiments with varying antibody:toxin molar ratios and pretreatment times are planned.

Summary

In summary, a high-affinity antiserum was successfully raised in a goat by immunization with a PbTx-3/BSA conjugate. This antiserum did not differentiate between PbTx-2 and PbTx-3, suggesting specificity for the polyether backbone structure of the molecule. A radioimmunoassay using this serum has been developed. Standard curves indicate a detection limit of 0.2–0.5 ng toxin in phosphate-buffered saline. Development of the assay for use in biological fluids or tissue extracts is underway. At least two of the three PbTx-3 metabolites produced in vitro by isolated rat hepatocytes (see above) cross-reacted strongly with this antiserum. This suggests use of this antiserum as a screen for exposure to PbTx-3 and other brevetoxins sharing the same backbone structure. This antiserum completely inhibited in vitro binding of [^{3}H]PbTx-3 to its receptor site in rat brain tissue, and blocked the in vivo pathophysiological effects of intravenous infusions of PbTx-2 when administered prophylactically. Studies to evaluate its therapeutic potential in the management of brevetoxin intoxication are underway.

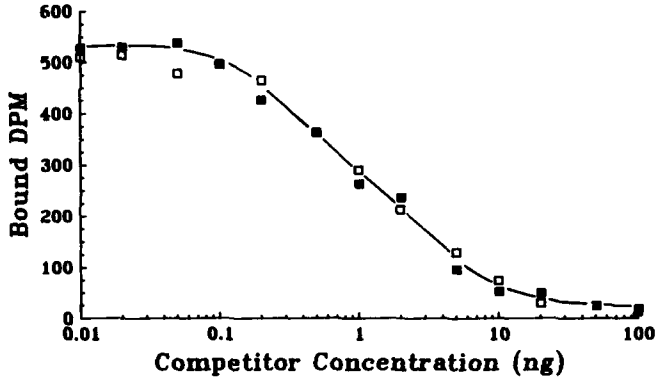

Figure 8. Standard curves for PbTx-2 (□) and PbTx-3 (■) in the brevetoxin radioimmunoassay. Lower detection limits are 0.2 – 0.5 ng in phosphate-buffered saline (PBS). Standard RIA conditions: [^{3}H]PbTx-3 = 1 nM; antiserum dilution = 1:2000; sample vol. ≈ 1 ml; buffer = 0.1 M PBS, pH = 7.4.

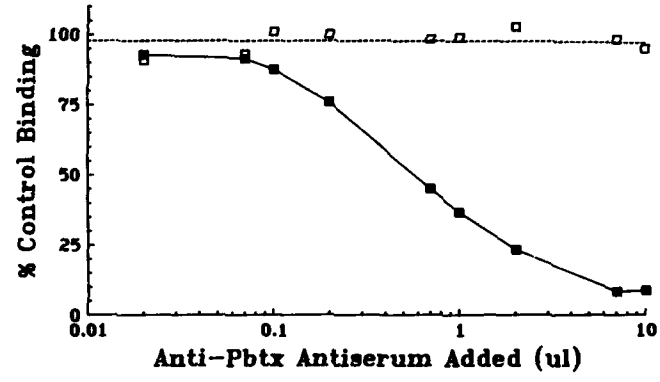

Figure 9. Anti-PbTx antiserum inhibition of [^{3}H]PbTx-3 binding to its receptor site in rat brain membrane preparations. Labeled toxin (0.5 nM in 1 ml PBS) was incubated with rat brain membranes (125 μg total protein) and increasing amounts of anti-PbTx antiserum (-■-) or pre-immune serum (-□-) for 1 hr at 4°C. Membrane-bound radioactivity was then measured in a centrifugation assay as previously described (*8*).

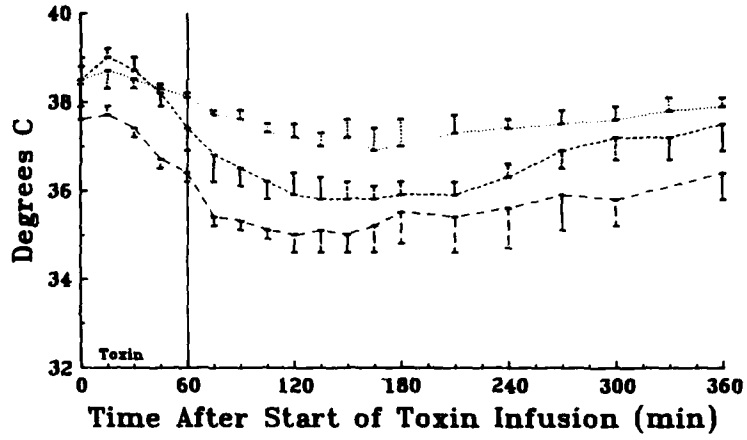

Figure 10. Response curves of core temperature for rats given 1-hr infusion of PbTx-2 (100 μg/kg) followed by a 10-min infusion of 2 ml of saline (———), 6:1 molar ratio of control antibody:toxin (---), or 6:1 molar ratio of anti-PbTx antibody:toxin (. . .).

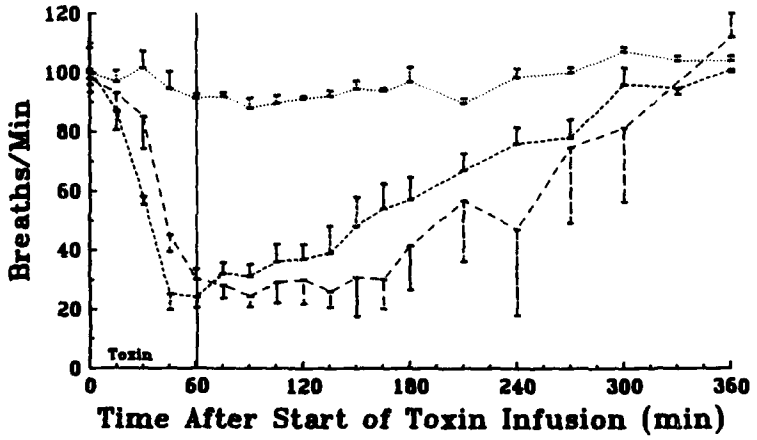

Figure 11. Response curves of respiratory rate for rats given 1-hr infusion of PbTx-2 (100 μg/kg) followed by a 10-min infusion of 2 ml of saline (———), 6:1 molar ratio of control antibody:toxin (---), or 6:1 molar ratio of anti-PbTx antibody:toxin (. . .).

Acknowledgments

The work of M.P. was performed during his tenure as a National Research Council Postdoctoral Associate at the United States Army Medical Research Institute of Infectious Diseases in Frederick, Maryland.

All procedures performed in this study conform to the "Guide to the Care and Use of Laboratory Animals" published by the National Institutes of Health, Bethesda, Maryland. All research facilities are accredited by the American Association for Accreditation of Laboratory Animal Care.

The opinions of the authors in no way reflect the opinions of the Department of the Army or the Department of Defense.

Literature Cited

1. Davis, C.C. *Bot. Gaz.* **1947**, *109*, 358–360.
2. Trieff, N.M.; Ramanujam, V.M.S.; Alam, M.; Ray, S.M. *Proc. 1st Intl. Conf. Toxic Dinoflagellate Blooms* **1975**, p 309–321.
3. Alam, M.; Trieff, N.M.; Ray, S.M.; Hudson, J. *J. Pharmaceut. Sci.* **1975**, *64*, 685.
4. Risk, M.; Lin, Y.Y.; MacFarlane, R.D.; Sadagopa-Ramanujam, V.M.; Smith, L.L.; Trieff, N.M. In *Toxic Dinoflagellate Blooms*; Taylor, D.L.; Seliger, H.H., Eds.; Elsevier North Holland: New York, **1979**; p 335–344.
5. Baden, D.G.; Mende, T.J.; Block, R. In *Toxic Dinoflagellate Blooms*; Taylor, D.L.; Seliger, H.H., Eds.; Elsevier North Holland: New York, **1979**; p 327–334.
6. Lin, Y.Y.; Risk, M.; Ray, S.M.; Van Engen, D.; Clardy, J.; Golik, J.; James, J.C.; Nakanishi. K. *J. Am. Chem. Soc.* **1981**, *103*, 6773–6774.
7. Shimizu, Y. *Pure Appl. Chem.* **1982**, *54*, 1973–1980.
8. Poli, M.A.; Mende, T.J.; Baden, D.G. *Mol. Pharmacol.* **1986**, *30*, 129–135.
9. Baden, D.G. *Int. Rev. Cyt.* **1983**, *82*, 99–149.
10. Steidinger, K.A.; Baden, D.G. In *Dinoflagellates*; Specter, D., Ed.; Academic: New York, **1984**; p 201–261.
11. Poli, M.A. Ph.D. Thesis, University of Miami, Florida, 1985.
12. Huang, J.M.C.; Wu, C.H.; Baden, D.G. *J. Pharmacol. Exp. Ther.* **1984**, *229*(2), 615–621.
13. Lombet, A.; Bidard, J.-N.; Lazdunski, M. **FEBS Lett. 1987**, *219(2)*, 355-359.
14. Risk, M.; Lin, Y.Y.; Ramanujam, S.; Smith, L.L.; Ray, S.M.; Trieff, N.M. *J. Chrom. Sci* **1979**, *17*, 400–405.
15. Whitefleet-Smith, J.; Boyer, G.L.; Schnoes, H.K. *Toxicon* **1986**, *24*, 1075–1090.
16. Pawlok, J.; Tempesta, M. S.; Golik, J.; Zagorski, M. G.; Lee, M.S.; Nakanishi, K.; Iwashita, T.; Gross, M.L.; Tomer, K.B. *J. Am. Chem. Soc.* **1986**, *109*, 1144–1150.
17. Nakanishi, K. *Toxicon* **1985**, *23*, 474–479.
18. Pace, J.G.; Watts, M.R.; Burrows, E.D.; Dinterman, R.E.; Matson, C.; Hauer, E.C.; Wannemacher, R.W., Jr. *Toxicol. Appl. Pharmacol.* **1985**, *80*, 337–385.
19. Baden, D.G.; Mende, T.J. *Toxicon* **1982**, *20*, 457–461.
20. Baden, D.G.; Mende, T.J.; Lichter, W.; Wellham, L. *Toxicon* **1981**, *19*, 455–462.
21. Chou, H.; Shimizu, Y. *Tetrahed. Lett.* **1982**, *23*, 5521–5524.
22. Golik, J.; James, J.C.; Nakanishi, K. *Tetrahed. Lett.* **1982**, *23*, 2535–2538.
23. Shimizu, Y.; Chou, H.; Bando, H. *J. Am. Chem. Soc.* **1986**, *108*, 514–515.
24. Poli, M.A. *J. Assoc. Off. Analyt. Chemists.* **1988**, *71(5)*, 1000-1002.
25. Poli, M.A. *Toxicon* **1988**, *26*, 36.
26. Dobson, E.L.; Jones, H.B. *Acta Med. Scand.* **1952**, *144* (Suppl. 273), 34.

27. Pace, J.G. *Fund. Appl. Toxicol.* **1986**, *7*, 424–433.
28. Pace, J.G.; Poli, M.A.; Canterbury, W.J.; Matson, C.F. *Pharmacologist* **1987**, *29*, 150.
29. Takitani, S.; Asabe, Y.; Kata, T.; Ueno, Y. *J. Chromatog.* **1979**, *172*, 335–342.
30. Rane, A.; Wilkinson, G.R.; Shand, D.G. *J. Pharmacol. Exp. Ther.* **1977**, *200*, 420–424.
31. Rowland, M. *Eur. J. Pharmacol.* **1972**, *17*, 352–356.
32. Templeton, C.B.; Poli, M.A.; LeClaire, R.D. *Toxicon* **1989**, in press.
33. Baden, D.G.; Mende, T.J.; Walling, J.; Schultz, D.R. *Toxicon* **1984**, *22*, 783–789.
34. Templeton, C.B.; Poli, M.A.; Solow, R. *Toxicon* **1989**, in press.

RECEIVED June 26, 1989

Reprinted from ACS Symposium Series No. 418
Marine Toxins: Origin, Structure, and Molecular Pharmacology
Sherwood Hall and Gary Strichartz, Editors